Science of the Total Environment 855 (2023) 158965

Contents lists available at ScienceDirect

Science of the Total Environment

journal homepage: www.elsevier.com/locate/scitotenv

Impact of needle-point bipolar ionization system in the reduction of bioaerosols in collective transport

Marta Baselga [a], Juan J. Alba [a,b], Alberto J. Schuhmacher [a,c,*]

[a] Institute for Health Research Aragon (IIS Aragón), 50009 Zaragoza, Spain
[b] Department of Mechanical Engineering, University of Zaragoza, 50018 Zaragoza, Spain
[c] Fundación Agencia Aragonesa para la Investigación y el Desarrollo (ARAID), 50018 Zaragoza, Spain

HIGHLIGHTS

- Collective transport is considered one of the environments with the highest rate of COVID-19 propagation.
- Air purification can reduce airborne transmitted diseases.
- Standard filters installed in trams present reduced efficiency for submicron particles.
- A bipolar ionization unit in a tram has been evaluated for the first time.
- Bipolar ionization can reduce environmental bioaerosols but not CFUs on surfaces.

GRAPHICAL ABSTRACT

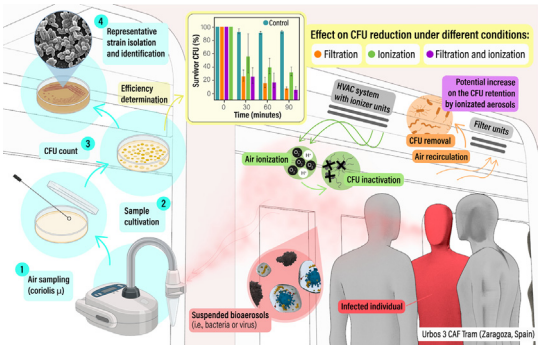

ARTICLE INFO

Editor: Warish Ahmed

Keywords:
Collective transport
Tramway
Bipolar ionization
Bioaerosols
Infectious diseases
SARS-CoV-2

ABSTRACT

The transmission rate of SARS-CoV-2 is higher in collective transport than in other public environments. Transport companies require preventive strategies to mitigate airborne risk of contagion which not imply responsible use at the individual level. Air purification systems, such as UV-C or needle-tip bipolar ionization, are attractive alternatives. However, only a few studies addressing the validation of this technology against bioaerosols in actual operation conditions have been published so far. In this work, the efficiency of a bipolar ionization unit in the Zaragoza Tram has been evaluated. Against environmental bioaerosols, ionization ($\sim 25.7 \cdot 10^9$ ions/m^3, on average) reduced the concentration of colony-forming units (CFU) by ~46 % and ~69 % after 30 and 90 min. No clear benefits were obtained against microorganisms on inner tram surfaces (seats, grab bars, walls, and windows). 'Pre-pandemic' filtration equipment located in the HVAC based on a Coarse 45 %-type filter removed ~73 and ~ 92 % of aerial CFU by itself after 30 and 90 min. Microscopic visualization of the CFUs revealed that they were mostly >1 μm, much larger than the SARS-CoV-2 virion (~100 nm) and SARS-CoV-2-loaded bioaerosols (from 0.25 μm). Then, we studied the filter behavior under normalized laboratory methods. The filters efficiency against submicron particles was limited (between 5 and 12 % against 0.1 to 0.3 μm NaCl particles). Another ionization strategy was to generate aerosol agglomerates to enhance filtration performance, but the combined action of ionization and filtration did not improve substantially. The effect of these technologies was also characterized using the clean air delivery rate (CADR). Relative to untreated air (CADR = 0.299 m^3/min), ionization and filtration reduce ambient CFUs (CADR = 5.153 and 9.261 m^3/min, respectively; and CADR = 13.208 m^3/min, combined) which implies that it has a substantial impact on indoor bioaerosols.

* Correspondence author at: Institute for Health Research Aragon (IIS Aragón), 50009 Zaragoza, Spain.
E-mail address: ajimenez@iisaragon.es (A.J. Schuhmacher).

http://dx.doi.org/10.1016/j.scitotenv.2022.158965
Received 26 April 2022; Received in revised form 12 September 2022; Accepted 19 September 2022
Available online 23 September 2022

1. Introduction

The airborne transmission model refers to the spread of a disease through aerosols up to 100 μm, which can be transmitted through the air over time and distance (Siegel et al., 2019). At the beginning of the COVID-19 pandemic, this route of infection was not considered relevant, and more attention was paid to the transmission through droplets and infected surfaces (Wang et al., 2021). The global acceptance of the spread of SARS-CoV-2 by aerosols allowed an improvement in the preventive approach, including new techniques for epidemiological management, such as the measurement of exhaled carbon dioxide (CO_2) as an indicator of the risk of contagion (Wang et al., 2021; Peng and Jimenez, 2021) and air purification technologies.

The term 'bioaerosol' refers to those particles of biological origin or active particles that can affect living organisms, causing them some allergy, toxicity, or infection (Rose, 1994, Sánchez-Monedero et al., 2006). Bioaerosols can include viruses, bacteria, spores, pollen, and, in general, any other microorganisms with an aerodynamic diameter between 0.5 and 100 μm (Cox and Wathes, 1995). In the context of airborne pathogen transmission, following mechanistic hypotheses about disease transmission, the spread of bioaerosols is associated with respiratory events (Hsiao et al., 2020), mainly coughs and sneezes (Asadi et al., 2019). However, the generation of bioaerosols has also been demonstrated during breathing and speech. Disseminating aerosols size ranges from a few nanometers to hundreds of micrometers (Asadi et al., 2019). Regarding the COVID-19 pandemic, bioaerosols released by a person infected with SARS-CoV-2 may contain some virus or traces of it, and the viral load contained in the particles is a crucial factor in determining the relative contribution of airborne transmission (Wang et al., 2021; Sattar and Ijaz, 1987). The modal distributions of aerosols acquire great relevance in infection transmission. Particle size determines the aerodynamic characteristics and deposition dynamics and the variability in the viral colonization model depending on the depth of the reached respiratory tract (Wang et al., 2021; Shinya et al., 2006; Guzman, 2021).

A higher transmission rate of SARS-CoV-2 has been observed in means of transport compared to other public and shared spaces. Thus, Lan et al., 2020 analyzed the relationship between the transmission of COVID-19 and the type of work, pointing to an incidence of 18 % of cases in the transport sector, only behind the health sector (22 %). Zhao et al., 2020 determined an association between the number of infected patients and the domestic transportation route of Wuhan by train, private car, and flights, finding a significant relationship between the infection rate and transportation by train, but not in flights and private vehicles. This trend was also studied using other infectious disease models (Horna et al., 2010, Troko et al., 2011, Goscé and Johansson, 2018).

The risk of contagion in public transport is determined by the seat's proximity to the infected person, the number of passengers, the number of interactions with other passengers, the duration of the trip, and the capacity performance of air renewal (Nasir et al., 2016). Generic measures have been adopted and have proven effective to reduce the virus spreading: surfaces sanitation, social responsibility measures (such as the use of a mask, social distancing, and hand hygiene), and ventilation measures (Moreno et al., 2021; Di Carlo et al., 2020). Regarding basic interior sanitation, solutions based on chlorine and isopropyl alcohol effectively disinfect surfaces (European Centre for Disease Prevention and Control (ECDC), 2020). Recommendations from the Centers for Disease Control and Prevention (CDC) and The Transportation Research Board (TRB) include at least two daily cleanings and suggest having particular account high-touch zones (American Public Transportation Association, 2020). The survival of SARS-CoV-2 varies depending on the material on which it is deposited. SARS-CoV-2 remains active for up to 72 h on plastic and stainless steel, up to 24 h on cardboard, and <4 h on copper (Van Doremalen et al., 2020), therefore it would be necessary to consider heterogeneity within the different areas of the same public transport unit.

HEPA filtration is very effective eliminating of microorganisms present in the ambient air in the means of transport since it allows efficient elimination of microorganisms reaching efficiencies close to 99.997 % (Askar et al., 2012; Leder and Newman, 2005). However, the performance of this technology will depend on the number of air changes and the feasibility of incorporating these filters to the installed air conditioning system. The percentage of recirculated air is another aspect to consider in the air quality in transport (Zitter et al., 2002). Additionally, natural air renovation, such as opening windows, can considerably reduce the concentration of CO_2 inside a vehicle as well as the number of airborne containing microorganisms (Matose et al., 2019). Concerning the COVID-19 pandemic, the preventive strategy to reduce the risk of contagion by aerosols has been managed along two different lines: on the one hand, based on the measurement of CO_2 as an indicator of air renovation. On the other hand, by purifying or cleaning the air by different means including ultraviolet C (UV-C) radiation technology, dry fumigation with hydrogen peroxide (H_2O_2) or technology based on non-thermal plasma, among others.

Technology based on the UV spectrum between 200 and 280 nm (UV-C) has been widely used in disinfection processes. The intracellular components of microorganisms (DNA, RNA, and proteins) present a high and variable sensitivity to absorb UV-C photons, producing critical damage to their genome and inhibiting their correct replication (Bolton and Cotton, 2008). The efficiency of UV disinfection varies depending on the distance from the surface and the application time (Li et al., 2017). This technology has proven helpful against the SARS-CoV-2 virus (Liang et al., 2021; Biasin et al., 2021; Ruetalo et al., 2021), reducing the viral load between 0 and 6 log orders of magnitude in culture media (Raeiszadeh and Adeli, 2020). Although the performance of the technology is limited against bioaerosols loaded with SARS-CoV-2, where the required UV_{254} dose is high (Raeiszadeh and Adeli, 2020), some studies highlight its effectiveness for air purification (Bowen et al., 2021) and especially if combined with HEPA filtration (Barnewall and Bischoff, 2021).

Non-thermal plasma-based technology has positioned itself as one of the leading air purification strategies in the context of the pandemic caused by the SARS-CoV-2 virus. Plasma inactivation of microorganisms has been attributed to cell wall rupture and damage of the genetic material (Liang et al., 2012). Its mechanism of action is multiple. The presence of charged particles, ions, reactive oxygen species (ROS) and oxygen-containing radicals, UV-C, vacuum ultraviolet (VUV), and localized heating events stand out, acting exclusively or in combination (Gallagher et al., 2007; Laroussi, 2007; Sakudo and Shintani, 2010; Nehra et al., 2008). The antimicrobial effect of this technology has been widely exploited in the health sector to sterilize surgical instruments (Klämpfl et al., 2012). Moreover, it has been tested in controlled environments reporting excellent efficiency in the inactivation of specific bacterial species (Liang et al., 2012) and enveloped/non-enveloped viruses (Sakudo et al., 2013; Sakudo et al., 2017; Sakudo et al., 2016). However, a limited number of studies support its efficiency in other settings.

Non-thermal plasma-based technology has been tested for other applications regarding the current pandemic, obtaining variable and lower results than those described by the manufacturers (Licht et al., 2021). One of the major concerns and limitations of this technology is the generation of by-products in harmful concentrations (Sleiman and Fisk, 2009), where some authors suggest increases in actual conditions (Zeng et al., 2021). However, this aspect is not discussed in this article. This work provides information on possible systems to reduce the risk of infectious diseases in public transport. First, the efficacy of needle-point bipolar ionization against eliminating environmental bioaerosols in the Zaragoza Tram (Zaragoza, Spain) is evaluated. Given biosafety and ethical constraints, we decided to perform the assays using environmental bacteria (not artificially dusted). Afterward, the efficiency of the isolated filtration media is tested against non-biological particles. These tests carried out in the laboratory allow the efficiency of the filter to be measured against submicron matter (hardly characterizable using the previous tests). Finally, the combined action of both strategies is studied. In parallel, the antimicrobial performance of ionization for surface disinfection is evaluated. This work evaluates the air purification systems for their implementation in local public transport.

2. Materials and methods

2.1. Needle-tip bipolar ionization system

As shown in Fig. 1, two PA604 ionization units of the 600 Series (Tayra SA, Spain) were installed in the suction vertices of the delivery fan of the two air conditioning units arranged in the Zaragoza Tram Unit (Model Urbos 3 CAF, ES). The two HVAC (Heating, Ventilation, and Air Conditioning) units installed in the Tram drive a total flow of 2800—3300 m^3/h, with a fresh air ratio of 1:3 fresh/return air. The selected ionizers were of the needle tip brush type (PA604, Tayra SA Spain). They produce an equal amount of positive and negative ions. They have a maximum treated flow of 4100 m^3/h and a <5 kV DC voltage between brushes. In the case of the tests where ionization was evaluated, an Air Ion Counter COM-3200PRO II (Com System INC, Tokyo JA) was used to ensure the correct generation of ions.

2.2. Conditions and preparation of the tram units

The Urbos 3 tram model (CAF, Spain) has a total length of 33 m, a width of 2.65 m, and a height of 3.2 m. It has a capacity of 200 seats, of which 146 are standing seats (3.5 people per m^2) and 54 are seats. It operates in Zaragoza, the fifth biggest city in Spain, with a population close to 700 k inhabitants, located midway between Madrid and Barcelona. The tram units included in the study were in operation for a full day, and the usual protocol was not carried out night cleaning. During the morning of the following day, the tram unit provided partial service lasting approximately 4 h. During this time, the hydroalcoholic gel dispensers were removed to avoid disinfection of the tram surfaces included in the study, and the windows were closed during the journeys. Travelers wore masks. Upon arrival at the depot, all the tram doors were opened for 15 min to renew the interior air and replace it with fresh ambient air. Doors opening were performed to maximize the homogeneity and reproducibility of the assays. The conditions used for the preparation of the Tram Units are detailed in Table 1.

The bipolar ionization units were turned on and stabilized for at least 15 min prior to the start of the test. The filter used during the tests was the usual one recommended by the manufacturer (Coarse 45 % according to UNE-EN ISO 16890, Merak Long Life Filter, Madrid SP). They were kept in the same usual conditions and were within the period of useful life determined by the manufacturer. The air conditioning system was kept off for the reference sampling, and the Tram was ventilated between tests, recirculating the depot air for at least 15 min.

2.3. Environmental sampling conditions and cultivation

A total of 6000 l of air was sampled at a flow rate of 300 l/min in an initial 5 ml of phosphate buffered saline (PBS) solution (Sigma-Aldrich, Darmstadt DE) using a Coriolis μ (Bertin Technologies, Montigny-le-Bretonneux FR). Sampling was carried out at three different points of the Tram to homogenize the sampling and collect microorganisms at points characterized by different ionic concentrations. The manufacturers initially modeled the ion concentration throughout the Tram Unit, guaranteeing a sufficient concentration for the inactivation of microorganisms in any of their locations. In each test, three samplings were carried out with a frequency of 30 min to evaluate the system's efficiency for 90 min, corresponding to the travel time in each tram line. In addition, an initial sampling was carried out to calculate the relative efficiency. Once the sampling was finished, the volume corresponding to 450 l of air sample aspiration was seeded on a Plate Count Agar (PCA) plate (Scharlab, Spain), for 72 h at 30 °C. The final sampled solution was variable depending on the climatological conditions of the sampling. Thus, the counts were normalized to be comparable, taking the environmental sampling prior to the intervention as a reference. Five replicates of each sample were made. Colony-forming units (CFU) were manually counted after the incubation period (72 h at 30 °C). The CFU counted in each replica were averaged and normalized. Efficiency in CFU inactivation was calculated by comparing the percentage of surviving CFUs with the reference sample.

Table 1
Set-up conditions established in each air sampling tests. Note that the HVAC A/C ventilation conditions have remained stable in all the samples.

Sampling conditions	Dampers	Filter	HVAC conditions	AFNPBI
Without ionization and filtration (stability test)	Closed	No	22 °C	No
Ionization	Closed	No	22 °C	Yes
Filtration	Closed	Yes	22 °C	No
Ionization and filtration	Closed	Yes	22 °C	Yes

2.4. Identification and visualization of the bacterial species found

Among the CFUs, the 15 most representative specimens collected during the samplings were analyzed. The identification of the microorganisms has been carried out using MALDI-TOF mass spectrometry technology (MALDI Biotyper, Bruker Massachusetts USA), comparing the results to databases (Bruker, Massachusetts USA). The morphology of the bacterial strains fibers was observed using a Scanning Electron Microscopy (SEM) JEOL 6360-LV (Deben UK Ltd., Edmunds, United Kindom). For sample preparation, a sample of the corresponding CFU was placed on a slide, fixed with carbon tape to a SEM microscope holder and sputtered with Au/Pd to promote electron conduction. The average of CFUs diameters and standard deviations (SD) were obtained from manual measurements with the free software Image-J (v1.52; Schindelin et al., 2012) for $n = 50$.

2.5. Sampling conditions of surfaces and cultivation

Rodac-PCA plates (Plate Count Agar-Sharlab, Spain) were used for surface sampling. At least 30 surface samples per test were taken at different points of the Tram, at different levels, and considering different types of

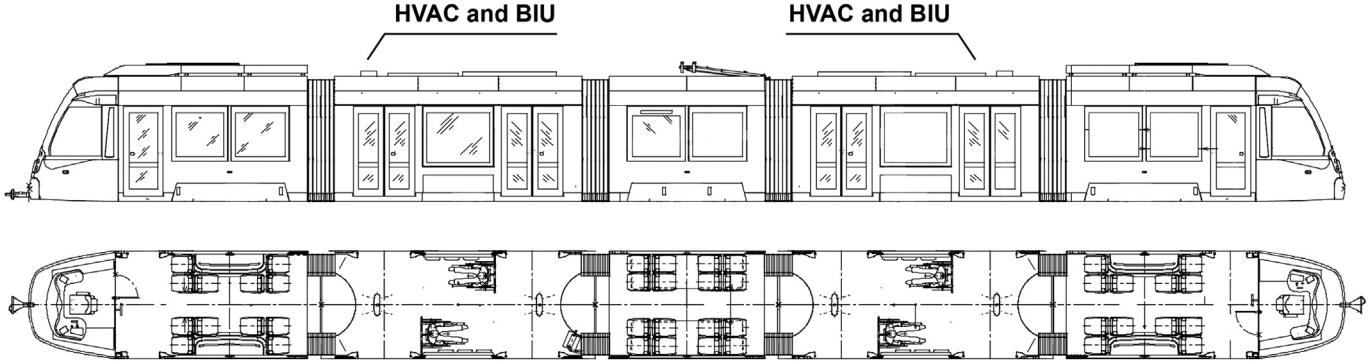

Fig. 1. Schematic representation of the bipolar ionization units and the HVAC systems ubication in the studied in the Urbos 3 tram model studied. Where the implementation of the BIU systems in the two HVAC is observed.

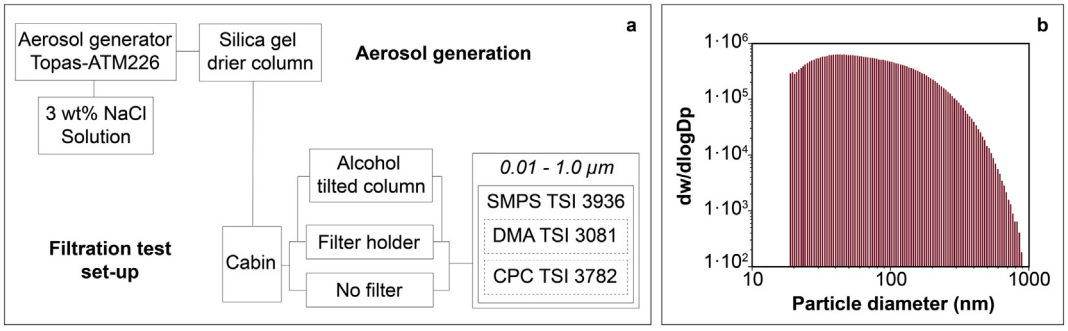

Fig. 2. a) Diagram of the equipment used to characterize the filters. b) Particle concentration distribution for efficiency determination measurements in the range.

surfaces. Seats, backrests, grab bars, intermediate supports, walls, and windows were included. Despite being carried out initially, the soil samples were excluded due to their high variability associated with residual contamination and dirt. The final surface sample was compared with a nearby (5 cm proximity) reference sample, and the ionization efficiency was calculated following the same method as for air sampling. Samples collected by contact in the Rodac-PCA plates were cultivated for 72 h at 30 °C.

2.6. Determination of filtration efficiency against submicron particles

As shown in Fig. 2-a, aerosols were produced using a Topas-ATM226 generator with a saline solution of sodium chloride (3 % NaCl in ddH_20). The obtained microdroplets pass through a tubular silica gel air dryer to evaporate the water and produce solid particles. The particle size distribution (Fig. 2-b) inside the cabin was measured using an SMPS TSI 3936 composed of an electrostatic classifier (DMA TSI 3081) and a condensation particle counter (CPC TSI 3782). The particles were dragged at a 0.6 l/min flow rate. The filter was placed between bronze discs sealed with Teflon tape, with 30 × 20 mm Teflon washers on each side. The exposed filter area was variable (2.05, 4.1, and 8.1 mm) to adjust the desired flow rate. The measurements lasted 2 min and were made in duplicate. Due to the concentration of particles variation, measurements were made passing through a free tube between measurements to calculate relative efficiency according to Eq. (1). Where C_{up} stands for concentration upstream and C_{down} stands for concentration downstream. The retention efficiency is expressed in global efficiency as 'number of particles'.

$$n = 100 \times \frac{C_{up} - C_{down}}{C_{up}} \quad (1)$$

Pressure drop testing was carried out using alcohol columns based on Bernoulli's principle. The free ends of the tubes have been inserted into the two quick couplings located on both sides of the filter sample holder. Measurements were made with a volumetric flow rate of 0.6 l/min.

2.7. Determination of air purification efficiency

System performance has been characterized using different approaches. Firstly, the calculation of the relative efficiency in the air and surface samples was carried out according to Eq. (2). The determination of the final CFU (CFU_2) was given as the average between the counts of the five replicates of each sampling. The initial CFU data (CFU_1) was taken from the previous test to assess performance every 30 min. Those cultures plates replicates with CFUs with values higher than three times those of the rest of the plates of the same sample were eliminated as they were considered non-representative extreme values. Secondly, clean air delivery rate (CADR) and first order loss rates using a simple linear regression against ln-transformed mean concentration values was determined as described by Stephens et al. (2022).

$$n = 100 \times \frac{CFU_1 - CFU_2}{CFU_1} \quad (2)$$

3. Results and discussion

3.1. Effect of filtration and needle-tip brush bipolar ionization on air

3.1.1. CFU stability in the environmental air

Airborne microorganisms are significantly affected by weather and environmental conditions (Fang et al., 2018; Zhang et al., 2017; Ehrlich et al., 1970). To guarantee a stable concentration of environmental bacteria during the tests, air samples were taken every 30 min without filtration and ionization. As depicted in Fig. 3, the results of this test suggest that the environmental microbiota is stable over time during the study hours on the same day. An average of 40.4 ± 1.5 CFU/m^3 of air was obtained during the first test and 53.8 ± 3.0 CFU/m^3 during the second test. CFU counts were averaged using all five replicates of each sample. In the plates at 30 and 90 min from the first test, 40.0 CFU/m^3 were counted in each one

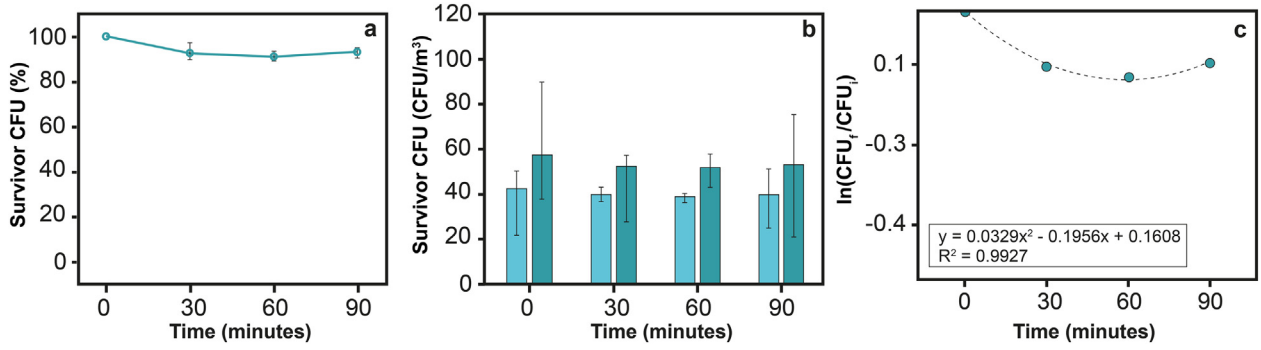

Fig. 3. a) Average percentage of survivor CFU. b) CFU/m^3 count of the two samples stability tests from the initial reference value. c) First-order loss rate constant regression in CFU stability tests.

Table 2
Results of the bacterial species identification. Where it is observed that they come mainly from human origin and are Gram positive in nature.

Ref	Strain	Score[a]	Gram	Average ± SD	Probable origin
S1	*Roseomonas mucosa*	1.76	Neg	3.5 ± 0.7 μm	Mucous (Romano-bertrand et al., 2016)
S2	*Micrococcus luteus*	2.13	Pos	1.2 ± 0.8 μm	Soil, dust, cutaneous (Kooken et al., 2014)
S3	*Tsukamurella paurometabola*	1.71	Pos	1.0 ± 0.1 μm	Pathogen (Munk et al., 2011)
S4	*Kocuria rhizophila*	1.77	Pos	0.9 ± 0.2 μm	Cutaneous (Takarada et al., 2008)
S5	Not identified	–	–	3.9 ± 0.5 μm	Not defined
S6	*Dermacoccus nishinomiyaensis*	1.75	Pos	1.1 ± 0.1 μm	Cutaneous (Williams and MacLea, 2019)
S7	*Microbacterium paludicola*	2.02	Pos	4.2 ± 1.3 μm	Not defined
S8	*Dermabacter hominis*	1.91	Pos	1.2 ± 0.2 μm	Cutaneous (Jones and Collins, 1988)
S9	*Roseomonas mucosa*	2.6	–	1.3 ± 0.2 μm	Mucous (Romano-bertrand et al., 2016)
S10	Not identified	–	–	1.1 ± 0.1 μm	Not defined
S11	*Staphylococcus haemolyticus*	2.1	Pos	0.9 ± 0.1 μm	Cutaneous (Eltwisy et al., 2020)
S12	*Deinococcus wulumuqiensis*	2.36	Pos	1.5 ± 0.2 μm	Not defined
S13	Not identified	2.0	–	1.0 ± 0.1 μm	Not defined
S14	*Bacillus cereus*	1.95	Pos	1.5 ± 0.2 μm	Not defined
S15	*Bacillus* sp.	–	Pos	3.5 ± 0.9 μm	Not defined

[a] The score indicates the effectiveness of the identification. Scores >2 indicate an excellent identification of the bacteria. Scores <2 indicate that the spectrum is related to the indicated bacterium but its concordance may not be exactly, so it could not be the indicated strain.

with respect to the initial 42.5 CFU/m^3. In the plates of the second test, 52.5 and 53.1 CFU/m^3 were found at 30 and 90 min, compared to the initial 57.5 CFU/m^3. To determine the stability of the CFUs, the Relative Standard Deviation (RSD) of each set of plates was calculated. The obtained RSD of ~0.04 in the first test and ~0.06 in the second test suggests that the bacterial environmental contamination is stable in air during the 90 min of sampling, so that the rest of the tests presented below are performed under robust and reproducible conditions throughout each test. Loss-rate regression of CFU has been fitted to a polynomial to characterize stability (Fig. 3c). The resulting CADR of 0.299 m^3/min and the loss rate constant of 0.0012 per minute during the stability control condition reinforces the previous conclusion about the stability of environmental CFUs.

3.1.2. Bacterial species identification

As enumerated in Table 2, the 15 most frequent colonies were isolated and identified. The bacterial identification is of interest since the efficiency of the BIU is evaluated predominantly for this subset of strains, despite the existence of others in a smaller proportion. In addition, its visualization allowed to evaluate its morphology and size, which is relevant for filtration studies. As depicted in Fig. 4, most bacterial strain (12/15) have sizes >1 μm in its longest dimension. The measured dimension represents the minimum size in which each strain of CFUs can be found in the air.

3.1.3. Bipolar ionization reduces aerial CFUs

The effect of ionization was considered exclusively to evaluate the single efficiency of the bipolar ionization unit. The objective of this study was to isolate the efficiency of the ion system and quantify the improvement that it supposes by itself in the absence of other perturbations, such as the filtration of the air conditioning system. An increasing efficiency was observed from the initial sampling to the final samplings. Ion concentration varied ($19.9 \cdot 10^9$—$31.5 \cdot 10^9$ ions/m^3) in all the samplings carried out due to the heterogeneity in the air distribution at the different points of

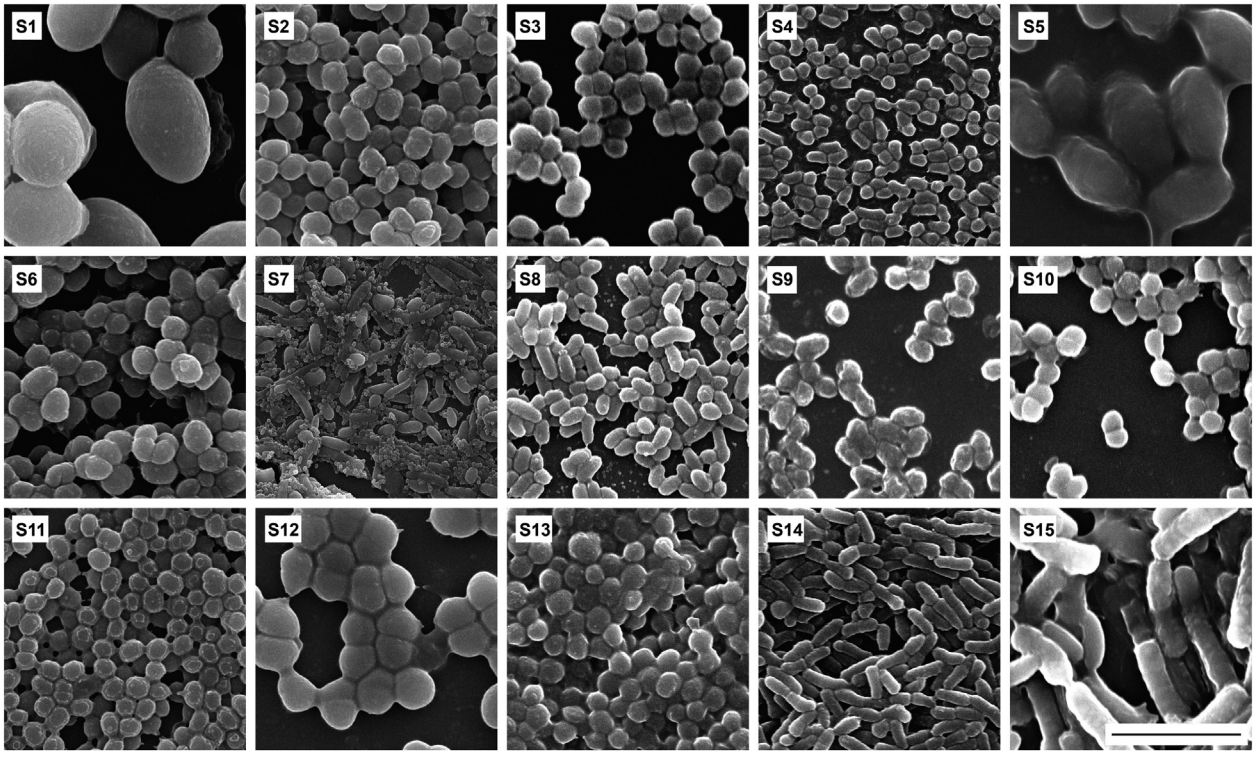

Fig. 4. Electron micrographs of isolated CFUs from air samples. Scale bar represents 5 μm for all images.

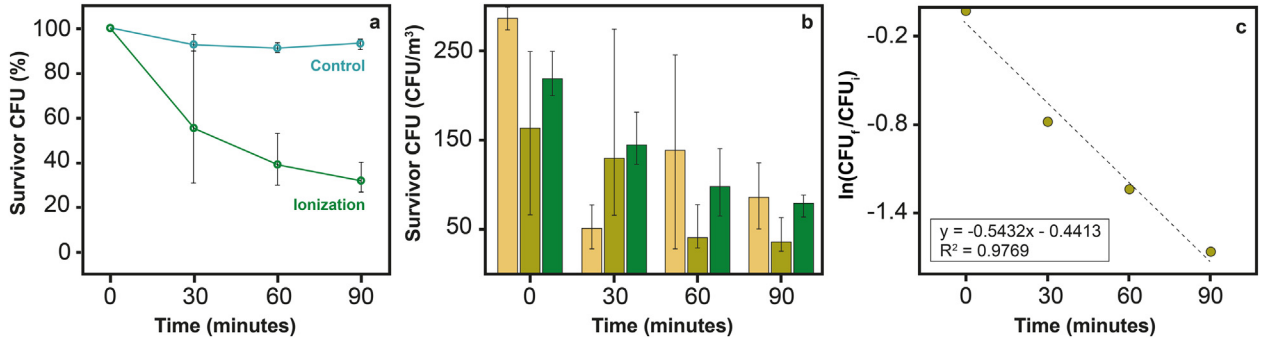

Fig. 5. a) Average percentage of survivor CFU. b) CFU/m^3 count of the three samples in ionization tests from the initial reference value. c) First-order loss rate constant regression in ionization inactivation tests.

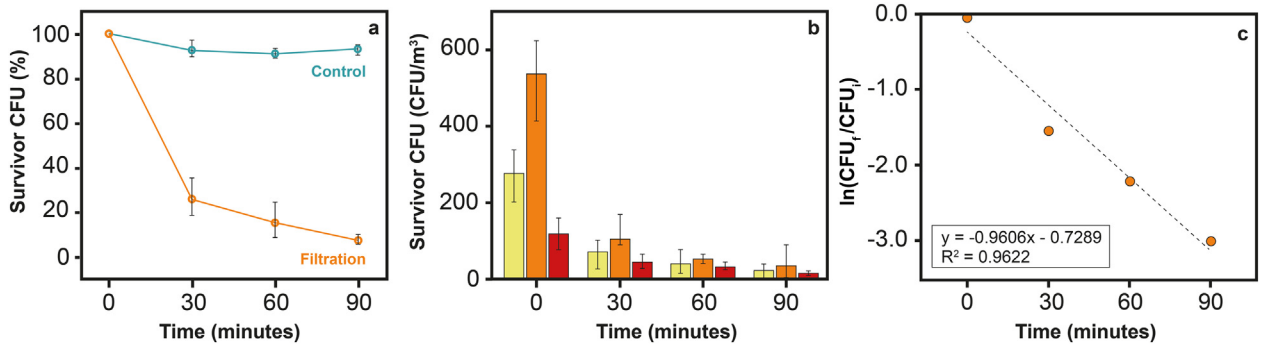

Fig. 6. a) Average percentage of survivor CFU. b) CFU/m^3 count of the three samples in filtration tests from the initial reference value. c) First-order loss rate constant regression in filtration inactivation tests.

the Tram. On average, during the first 30 min of the experiment, CFUs were reduced by 45.9 % (54.1 % persisted). As shown in Fig. 5, an efficiency of 61.8 % (38.2 % persisted) was estimated after 60 min. The efficiency increased to 69.2 % (30.8 % persisted) after 90 min. Licht et al., 2021 evaluated the efficiency of needle-point bipolar ionization systems (~10—20 kV) in airplanes, obtaining a reduction of CFU (*Staphylococcus epidermidis*) variable between 20.7 % and 60.0 % after 1 h of ionization, which is consistent with the results obtained in the present study. The resulting loss rate constant is 0.018 per minute under ionization conditions, and the estimated CADR was 5.153 m^3/min. Regarding the control values, it is observed that the clean air delivery rate increases, which implies a greater amount of air free of bioaerosols. Specifically, this value increased in >17 times.

3.1.4. Filtration reduces aerial CFUs

The electrostatic potential influence of the surface on the deposition of bacteria from the air has been demonstrated (Meschke et al., 2009). Various studies suggest that bipolar ionization reduces particulate matter in the air due to increased particle deposition and/or filtration efficiency associated with the increase in the aerodynamic diameter of aerosols due to the agglomeration of fine particles (Pushpawela et al., 2017; Wu et al., 2015; Zeng et al., 2021). This phenomenon is mainly associated with electrostatic effects (Mayya et al., 2004; Grabarczyk, 2001) and is dependent on particle size and composition, relative humidity, ionization time, and surface material (Grabarczyk, 2001). Filters can interfere in estimating the efficiency of the ionization system. Then, the effect of the filtration implemented in the air conditioning system of the Tram has been characterized separately. The tests were carried out with the filter usually installed on the Tram (Coarse 45 % filter medium). The Air Changes per Hour (ACH) of the Zaragoza Tram remained as they are in the normal operation of the unit at 25 ACH. This indicates that the air passes through the filter 12.5 times/h on average. As seen in Fig. 6, loss rate constant was 0.033 per minute, and the estimated CADR was 9.261 m^3/min. These parameters imply that filtration is more effective than ionization. CFU amount upon filtration suggests a reduced efficiency considering the number of air changes inside the tram unit. On average, CFUs were reduced by 73.4 % (26.6 % persisted), 84.0 % (16.0 % persisted), and 92.0 % (8.0 % persisted) during the first 30, 60, and 90 min, respectively. In this sense, the CFUs are large enough to favor the filtration mechanisms since they are, for the most part, >1 μm.

Faced with submicron particles, smaller in size than the bacteria tested, the efficiency of the filter is limited according to the conditions studied (Table 3). The filter complies with the UNE-EN 16890 standard and refers to a 75 % filtration for particles greater than ~10 μm. This filter is efficient for the retention of dust or pollen. However, it is inefficient against fine particles and viruses. The tests carried out are limited. Due to the conditions of the equipment used for the determination of filtration efficiency against submicron particles, the filter may have been 'clogged' by the concentration of NaCl particles, assuming a notable increase in pressure drop and an ornament in the efficiency result. The Coarse 45 % filter was evaluated in a more compact format than natural: 2—3 mm thick instead of 20—30 mm. The results suggest that the speed at which the air passes through the filter medium retains the larger particles. However, no notable difference is observed in the flows studied. The curves could not be very representative of this filter's actual efficiency (in working conditions in the air conditioning system of the Tram).

Table 3
Laboratory conditions used in the filtration tests.

	Area (cm^2)	Flow (m^3/h)	Speed (cm/s)
Coarse 45 % filter	3740	~261.2	19.4
		~1019.2	75.7
		~4079.6	303.0

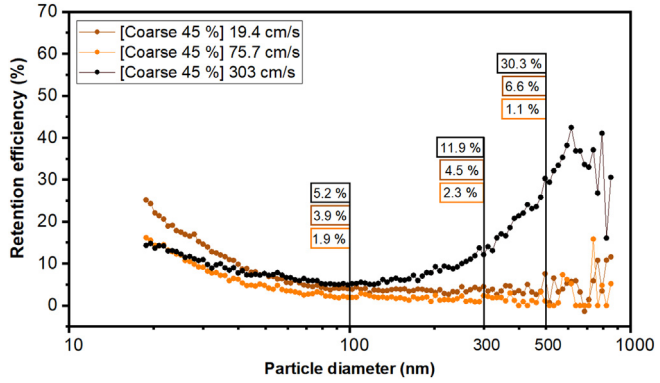

Fig. 7. Coarse 45 % filter retention efficiency depending on the particle diameter at different velocity in filter (flow rates). Where it is observed that the efficiency is dependent on the flow rate and the particle size.

Table 4
Pressure drop obtained from the Coarse 45 % filter. Where it is shown that pressure drop depends on the flow rate (measured as velocity in filter).

Velocity in filter (cm/s)	Pressure drop (Pa)
	Coarse 45 % filter
19.4	~6
75.7	~40
303.0	~380

In experimental sampling tests, SARS-CoV-2 viral RNA has been mainly found in particle sizes from 0.25 μm (Kenarkoohi et al., 2020; Liu et al., 2020). Therefore, determining the efficiency of the filter against submicronic sizes and above is relevant to quantify its performance. As shown in Fig. 7, the Coarse 45 % filter presented an approximate retention efficiency of ~30 % for 0.5 μm particles at a flow rate of ~4079 m^3/h. For flow rates lower than this, the efficiency of the filter decreases to values <7 %. These tests suggest that larger particles have more inertia at high speeds (high flow rates) and, therefore, a higher retention rate in the filter medium (Yeh and Liu, 1974a, 1974b). However, the clogging of NaCl particles observed in the head loss tests may have overestimated these results. In the tests where the highest speed is simulated, clogging is observed, which translates into an increase up to 380 Pa of pressure drop (Table 4).

3.1.5. Effect of combined ionization and filtration efficiency against aerial CFUs

Once the effects of ionization and filtration were evaluated separately, the combination's performance was intended to study. However, no clear advantage was obtained from the combination of mechanisms. The first 30 min reduced the CFU concentration by 74.2 % (25.8 % persisted), while at 60 min, the efficiency increased to 82.8 % (17.2 % persisted), and at 90 min, 94.1 % was eliminated (5.9 % persisted) (Fig. 8). While these data are promising, the filtration alone reduced the CFU concentration by 73.4 % and 92.0 %, respectively, after 30 and 90 min. The maintenance of filtration efficiency can be explained because the highest rate of particle agglomeration due to electrostatic phenomena occurs in the finest particles (<0.15 μm). Then, there is a higher concentration of particles >0.3 μm (Zeng et al., 2021), which does not favor the performance of filtration (Yeh and Liu, 1974a, 1974b).

The loss rate constant was 0.047 per minute, and the estimated CADR was 13.208 m^3/min. The value of CADR of ionization and filtration together was higher than filtration and ionization separately by 3.947 and 8.055 m^3/min, respectively.

Table 5
Results of surface stability tests. Where, CFU_i refers to the CFU count in initial (t = 0) samples and CFU_f to final (t = 2 h) samples CFU counts.

Test	RSD (average)	$CFU_i = CFU_f$	$CFU_i < CFU_f$	$CFU_i > CFU_f$
Test 1	0.39	39.3 %	21.4 %	39.3 %
Test 2	0.64	17.2 %	58.6 %	24.2 %
Test 3	0.39	23.1 %	30.8 %	46.1 %
Test 4	0.61	13.3 %	33.3 %	53.4 %

CFU_i = Initial CFU; CFU_f = Final CFU.

3.2. Effect of the bipolar ionization in the elimination of CFUs on surfaces

3.2.1. Evaluation of the CFUs stability on surfaces

To guarantee the uniformity of the tests, four surface samples have been carried out, with a total of at least 60 Rodac PCA plates per test: 30 at $t = 0$ (CFU_i) and 30 at $t = 2$ h (CFU_f). Ideally, the CFU_i should be equal to the CFU_f (ie the percentage of CFUi = CFUf would ideally be 100 %). However, we have considered it relevant to analyze whether there are more or fewer CFU at the end of the experiment to determine if it is a matter of stability or simply variability across the surface (i.e., $CFU_i < CFU_f$ or $CFU_i > CFU_f$). If the CFUs had deteriorated over time, a trend greater than $CFU_i > CFU_f$. This has not been observed, so it is assumed that the CFUs are stable during the time of the experiment (2 h) but there is a non-negligible need between the neighboring test surfaces. To quantify this dispersion, the RSD of each set of plates has been calculated. RSD close to zero suggests high uniformity in the samples. The variability of the results (Table 5) required an increase in the sample to obtain representative conclusions.

3.2.2. Bipolar ionization efficiency on surface samples

On the one hand, "effectiveness" refers to the percentage of PCA plates where final CFU number was lower than the initial ($CFU_i > CFU_f$). That is, in this column the percentage of CFU plates that showed a potential action of ionization has been studied. On the other hand, "efficiency" represents the percentage of "removed" bacteria in these plates potentially due to ionization effect, which is calculated according to Eq. (2). It is relevant to differentiate between the efficiency for plates with CFU > 50, CFU > 20, and CFU > 10 to avoid distorting the results obtained. However, the global efficiency does not discriminate between values obtained (Table 6).

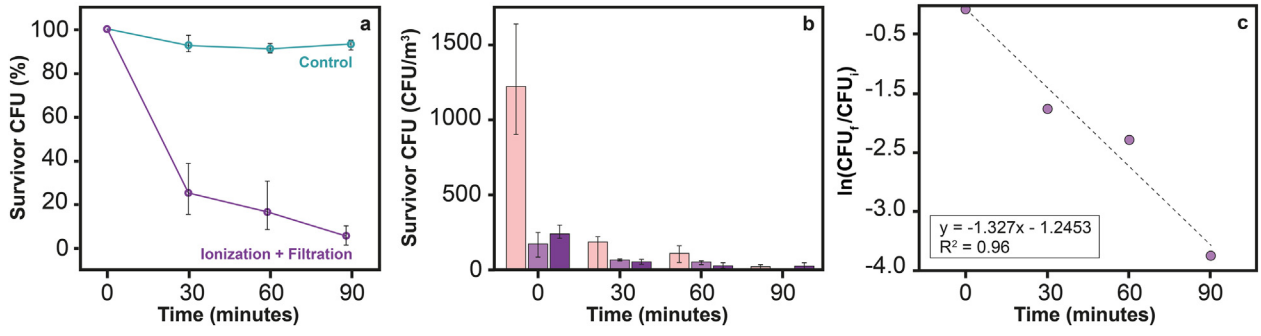

Fig. 8. a) Average percentage of survivor CFU. b) CFU/m^3 count of the three samples in simultaneous ionization and filtration tests from the initial reference value. c) First-order loss rate constant regression in both ionization and filtration inactivation tests.

Table 6
Effect of bipolar ionization tests on surfaces. Where, CFU_i refers to the CFU count in initial ($t = 0$) samples and CFU_f ($t = 2$ h) to final samples CFU counts.

Test	Effectiveness ($CFU_i > CFU_f$)	Global efficiency	Efficiency CFU > 50	Efficiency CFU > 20	Efficiency CFU > 10
Test 1	60 %	65.1 %	65.9 %	72.1 %	66.6 %
Test 2	53 %	44.0 %	43.4 %	36.3 %	40.9 %
Test 3	30 %	54.6 %	38.6 %	47.7 %	46.3 %
Test 4	53 %	73.0 %	65.9 %	78.4 %	73.0 %
Test 5	42 %	78.1 %	73.4 %	70.5 %	78.1 %
Test 6	40 %	81.4 %	69.2 %	83.6 %	81.4 %

CFU_i = Initial CFU; CFU_f = Final CFU.

According to our findings, in this experimental set-up, the ionization did not present a major role on the inactivation of microorganisms on surfaces. The average ionization effectiveness was 46 %, while the average $CFU_i > CFU_f$ in the stability study was 36 %. We cannot exclude that the difference between initial and final CFUs could be due to effects other than ionization.

4. Conclusions

The increasing understanding of the mechanisms behind COVID-19 infection transmission should drive a shift in the way we address the prevention of the transmission of this disease and other respiratory infections. A higher transmission rate of SARS-CoV-2 has been observed in transport compared to other public and shared spaces. It is required to implement preventive measures for different transportation settings and countries. In previous studies we found that the Zaragoza Tram did not represent a high risk of contagion (for more information see Baselga et al., 2022). Nevertheless, after the pandemic, preventive strategies are relaxed and the potential risk of contagion increases, so it is necessary to find long-term solutions for the improve the quality of the air we breathe. Although masks are very efficient in expelling fewer potentially pathogenic microorganisms into the air, it is a temporary measure that probably will not be used indefinitely.

Studies on environmental bioaerosols in air samples suggest that BIU systems have a beneficial effect on eliminating CFUs. The main limitation for the implantation of ionization systems is a possible generation of by-products due to the electrostatic interaction between elements, although this aspect is not discussed here, and it is out of the scope of this work. Under the conditions studied, which are favorable (including closed tram unit and long exposure times), efficiencies close to 69.2 % were obtained after 90 min of ionization. The implemented filtration system offers better results in the same period against microorganisms present in the air (92.0 %). The combined action of both systems slightly improved the filtration performance (94.1 %), not representing a major improvement. According to the literature, the predominance of agglomerates is close to 300 nm. However, the Tram filters tested in this study did not perform well in laboratory analyses against those particle sizes (<10 %). We cannot exclude a synergy of bipolar ionization with other filter types that could retain these agglomerates.

The filtration tests assayed in the studied Tram units are not very efficient for submicron particles. The Coarse 45 %-type filters are designed to eliminate dust, pollen, and larger particles. However, considering the number of air changes per hour (~25 ACH, ~1450 m^3/h) approximately 6 % of the CFUs are retained each time the air passes through the filter leading to a ~75 % efficiency observed during the first half-hour (note that no CFU sources existed during the tests). In addition, the main bacterial families found almost always presented sizes >1 um, so the filtration of submicron matter would be more representative in the case of viruses. A limited filtration of fine particles is observed in the tests carried out with submicron particles, where the retention of 0.1 μm particles was <6 %. Faced with these sizes, HEPA filters are an effective strategy. However, it must be considered that the quality of the filter is as important as its performance (measured in m^3/h). This is why the implementation of HEPA filters in the HVAC system of the Tram is unthinkable due to its pressure drop. Installation of stand-alone HEPA purification systems to reduce airborne CFUs and viruses could be considered, although this would require separate studies.

Through the technical feature recently agreed upon by the American Society of Heating, Refrigerating and Air-Conditioning Engineers (ASHRAE), it was possible to quantify the impact of the technologies (ionization and filtration) on the interior air of the Tram. It was performed using the loss rate value and the CADR parameter. Combined action of ionization and filtration (CADR = 13.208 m^3/min) present a substantially advantage over untreated air (CADR = 0.299 m^3/min). Even so, the filtration was also effective on its own (CADR = 9.261 m^3/min). Exclusive ionization did not have such a notable effect (CADR = 5.153 m^3/h), although also reduced the aerial CFU concentration.

All the assays described here were performed under favorable conditions for air purification since there was no external dissemination of bioaerosols and the air was constantly recirculated. Of note, our findings highlight the importance of filtration and air cleaning in public transport. Importantly, the development and validation of new effective air purification systems may be essential for minimizing the spread of infectious diseases in the future and this field merits further research.

Data availability

No data was used for the research described in the article.

Declaration of competing interest

The authors declare that they have no known competing financial interests or personal relationships that could have appeared to influence the work reported in this paper.

Acknowledgments

We would like to acknowledge to Los Tranvías de Zaragoza S.E.M. and CAF Spain S.A. for requesting this project and their invaluable collaboration throughout it. Authors also thank to the IIS Aragón and Liftec (CSIC) for their support. Authors would also like to acknowledge the use of Servicio General de Apoyo a la Investigación-SAI, Universidad de Zaragoza.

References

American Public Transportation Association, 2020. Cleaning and Disinfecting Transit Vehicles and Facilities During a Contagious Virus Pandemic.
Asadi, S., Wexler, A.S., Cappa, C.D., Barreda, S., Bouvier, N.M., Ristenpart, W.D., 2019. Aerosol emission and superemission during human speech increase with voice loudness. Sci. Rep. 9, 2348. https://doi.org/10.1038/s41598-019-38808-z.
Askar, M., Mohr, O., Eckmanns, T., Krause, G., Poggensee, G., 2012. Quantitative assessment of passenger flows in Europe and its implications for tracing contacts of infectious passengers. Eurosurveillance 17 (24), 20195. https://doi.org/10.2807/ese.17.24.20195-en.
Barnewall, R., Bischoff, W., 2021. Removal of SARS-CoV-2 bioaerosols using ultraviolet air filtration. Infect. Control Hosp. Epidemiol. 42, 1014–1015. https://doi.org/10.1017/ice.2021.103.
Baselga, M., Alba, J.J., Schuhmacher, A.J., 2022. The control of metabolic CO2 in public transport as a strategy to reduce the transmission of respiratory infectious diseases. Int. J. Environ. Res. Public Health 19 (11), 6605. https://doi.org/10.3390/ijerph19116605.
Biasin, M., Bianco, A., Pareschi, G., Cavalleri, A., Cavatorta, C., Fenizia, C., Galli, P., Lessio, L., Lualdi, M., Tombetti, E., Ambrosi, A., Redaelli, E.M.A., Saulle, I., Trabattoni, D., Zanutta, A., Clerici, M., 2021. UV-C irradiation is highly effective in inactivating SARS-CoV-2 replication. Sci. Rep. 11, 1–7. https://doi.org/10.1038/s41598-021-85425-w.
Bolton, J.R., Cotton, C.A., 2008. The Ultraviolet Disinfection Handbook. 1st Ed. American Water Works Association.
Bowen, R.A., Gilgunn, P., Hartwig, A.E., Mullen, J., 2021. Prevention of airborne transmission of SARS-CoV-2 by UV-C illumination of airflow. Covid 1 (3), 602–607. https://doi.org/10.3390/covid1030050.
Cox, C., Wathes, C., 1995. Bioaerosols Handbook.
Di Carlo, P., Chiacchiaretta, P., Sinjari, B., Aruffo, E., Stuppia, L., De Laurenzi, V., Di Tomo, P., Pelusi, L., Potenza, F., Veronese, A., Vecchiet, J., Falasca, K., Ucciferri, C., 2020. Air and surface measurements of SARS-CoV-2 inside a bus during normal operation. PLoS One 15, e0235943. https://doi.org/10.1371/journal.pone.0235943.
Ehrlich, R., Miller, S.O.L., Walker, R.L., 1970. Relationship between atmospheric temperature and survival of airborne bacteria. Appl. Microbiol. 19, 245–249. https://doi.org/10.1128/am.19.2.245-249.1970.

Eltwisy, H.O., Abdel-fattah, M., Elsisi, A.M., Omar, M.M., Aly, A., 2020. Pathogenesis of Staphylococcus haemolyticus on primary human skin fibroblast cells. Virulence 11, 1142–1157. https://doi.org/10.1080/21505594.2020.1809962.

European Centre for Disease Prevention and Control (ECDC), 2020. Considerations for infection prevention and control measures on public transport in the context of COVID19. Stockholm. Available online: https://www.ecdc.europa.eu/sites/default/files/documents/COVID-19-public-transport-29-April-2020.pdf. (Accessed 23 September 2022).

Fang, Z., Guo, W., Zhang, J., Lou, X., 2018. Influence of heat events on the composition of airborne bacterial communities in urban ecosystems. Int. J. Environ. Res. 15, 2295. https://doi.org/10.3390/ijerph15102295.

Gallagher, M.J., Vaze, N., Gangoli, S., Vasilets, V.N., Gutsol, A.F., Milovanova, T.N., Anandan, S., Murasko, D.M., Fridman, A.A., 2007. Rapid inactivation of airborne bacteria using atmospheric pressure dielectric barrier grating discharge. IEEE Plasma Sci. 35, 1501–1510. https://doi.org/10.1109/TPS.2007.905209.

Goscé, L., Johansson, A., 2018. Analysing the link between public transport use and airborne transmission: mobility and contagion in the London underground. Environ. Health 17, 84. https://doi.org/10.1186/s12940-018-0427-5.

Grabarczyk, Z., 2001. Electiveness of indoor air cleaning with coronaionizers. J. Electrost. 51, 278–283. https://doi.org/10.1016/S0304-3886(01)00058-4.

Guzman, M., 2021. An overview of the effect of bioaerosol size in coronavirus disease 2019 transmission. Int. J. Health Plann. Manag. 36 (2), 257–266.

Horna, O., Bedoya, A., Romero, N., Martín, M., 2010. Risk of tuberculosis in public transport sector workers, Lima, Peru. Int. J. Tuberc. Lung Dis. 14, 714–719.

Hsiao, T.C., Chuang, H.C., Griffith, S.M., Chen, S.J., Young, L.H., 2020. COVID-19: an aerosol. s point of view from expiration to transmission to viral-mechanism. Aerosol Air Qual. Res. 20, 905–910. https://doi.org/10.4209/aaqr.2020.04.0154.

Jones, D., Collins, M., 1988. Taxonomic studies on some human cutaneous coryneform bacteria: description of Dermabacter hominis gen.nov., sp.nov. FEMS Microbiol. Lett. 51, 51–55.

Kenarkoohi, A., Noorimotlagh, Z., Falahi, S., Amarloei, A., Abbas, S., 2020. Hospital indoor air quality monitoring for the detection of SARS-CoV-2 (COVID-19) virus. Sci. Total Envion. 748, 141324. https://doi.org/10.1016/j.scitotenv.2020.141324.

Klämpfl, T.G., Isbary, G., Shimizu, T., Li, Y., Zimmermann, J.L., Stolz, W., Morfill, G.E., Schmidt, H., 2012. Cold atmospheric air plasma sterilization against spores and other microorganisms of clinical interest. Appl. Environ. Microb. 78, e5077–e5082. https://doi.org/10.1128/AEM.00583-12.

Kooken, J.M., Fox, K.F., Fox, A., 2014. Characterization of micrococcus strains isolated from indoor air. Mol. Cell. Probes 26, 1–5. https://doi.org/10.1016/j.mcp.2011.09.003.

Lan, I., Wei, C., Id, Y.H., Christiani, D.C., 2020. Work-related COVID-19 transmission in six Asian countries/areas: a follow-up study. PLoS One 15, e0233588. https://doi.org/10.1371/journal.pone.0233588.

Laroussi, M., 2007. Low temperature plasma-based sterilization: overview and stateof-the-art. T Plasma Sci 35, e1501–e1510. https://doi.org/10.1002/ppap.200400078.

Leder, K., Newman, D., 2005. Respiratory infections during air travel. Intern. Med. J. 35, 50–55. https://doi.org/10.1111/j.1445-5994.2004.00696.x.

Li, Y., Wang, M., Guan, D., Lv, H., Zhao, J., Yu, X., Yang, X., Wu, C., 2017. A study on the decontaminated efficiency of ultraviolet device on the indoor airborne bacteria. Procedia Eng. 205, 1376–1380. https://doi.org/10.1016/j.proeng.2017.10.281.

Liang, Y., Wu, Y., Sun, K., Chen, Q., Shen, F., Zhang, J., Yao, M., Zhu, T., Fang, J., 2012. Rapid inactivation of biological species in the air using atmospheric pressure nonthermal plasma. Environ. Sci. Technol. 46, 3360–3368. https://doi.org/10.1021/es203770q.

Liang, J.J., Liao, C.C., Chang, C.S., Lee, C.Y., Chen, S.Y., Huang, S.B., Yeh, Y.F., Singh, K.J., Kuo, H.C., Lin, Y.L., Lu, K.M., 2021. The effectiveness of far-ultraviolet (UVC) light prototype devices with different wavelengths on disinfecting SARS-CoV-2. Appl. Sci. 11, 10661. https://doi.org/10.3390/app1122 10661.

Licht, S., Hehir, A., Trent, S., Dunlap, D., Borumand, K., Wilson, M., Smith, K., 2021. Use of Bipolar Ionization for Disinfection Within Airplanes.Available on: (accessed on 07/27/2022) https://www.boeing.com/confident-travel/downloads/Boeing-Use-of-Bipolar-Ionization-for-Disinfection-within-Airplanes.pdf.

Liu, Yuan, Ning, Z., Chen, Y., Guo, M., Liu, Yingle, Gali, N.K., Sun, L., Duan, Y., Cai, J., Westerdahl, D., Liu, X., Xu, K., Ho, K.Fai, Kan, H., Fu, Q., Lan, K., 2020. Aerodynamic analysis of SARS-CoV-2 in two Wuhan hospitals. Nature 582, 557–560. https://doi.org/10.1038/s41586-020-2271-3.

Matose, M., Poluta, M., Douglas, T., 2019. Natural ventilation as a means of airborne tuberculosis infection control in minibus taxis. S. Afr. J. Sci. 115, 1–4. https://doi.org/10.17159/sajs.2019/5737.

Mayya, Y.S., Sapra, B.K., Khan, A., Sunny, F., 2004. Aerosol Removal by Unipolar Ionization in Indoor Environments. 35, pp. 923–941. https://doi.org/10.1016/j.jaerosci.2004.03.001.

Meschke, S., Smith, M., Miksch, R., Gefter, P., Gehlke, S., Halpin, H., 2009. The effect of surface charge, negative and bipolar ionization on the deposition of airborne bacteria. J. Appl. Microbiol. 106, 1133–1139. https://doi.org/10.1111/j.1365-2672.2008.04078.x.

Moreno, T., Pintó, R.M., Bosch, A., Moreno, N., Alastuey, A., Minguillón, M.C., Anfruns-Estrada, E., Guix, S., Fuentes, C., Buonanno, G., Stabile, L., Morawska, L., Querol, X., 2021. Tracing surface and airborne SARS-CoV-2 RNA inside public buses and subway trains. Environ. Int. 147, 106326. https://doi.org/10.1016/j.envint.2020.106326.

Munk, A.C., Lapidus, A., Lucas, S., Nolan, M., Tice, H., Glavina, T., Rio, D., Goodwin, L., Pitluck, S., Liolios, K., 2011. Complete genome sequence of Tsukamurella paurometabola type strain. Stand. Genomic Sci. 4, 342–351. https://doi.org/10.4056/sigs.1894556.

Nasir, Z.A., Campos, L.C., Christie, N., Colbeck, I., 2016. Airborne biological hazards and urban transport infrastructure: current challenges and future directions. Environ. Sci. Pollut. Res. 23, 15757–15766. https://doi.org/10.1007/s11356-016-7064-8.

Nehra, V., Kumar, A., Dwivedi, H., 2008. Atmospheric non-thermal plasma sources. Int. J. Eng. 2, 53–68.

Peng, Z., Jimenez, J.L., 2021. Exhaled CO2as a COVID-19 infection risk proxy for different indoor environments and activities. Environ. Sci. Technol. Lett. 8, 392–397. https://doi.org/10.1021/acs.estlett.1c00183.

Pushpawela, B., Jayaratne, R., Nguy, A., Morawska, L., 2017. Efficiency of ionizers in removing airborne particles in indoor environments. J. Electrost. 90, 79–84. https://doi.org/10.1016/j.elstat.2 017.10.002.

Raeiszadeh, M., Adeli, B., 2020. A critical review on ultraviolet disinfection systems against COVID-19 outbreak: applicability, validation, and safety considerations. ACS Photon. 7, 2941–2951. https://doi.org/10.1021/acsphotonics.0c01245.

Romano-bertrand, S., Bourdier, A., Aujoulat, F., Michon, A., Masnou, A., Parer, S., Marchandin, H., Jumas-bilak, E., 2016. Skin microbiota is the main reservoir of Roseomonas mucosa, an emerging opportunistic pathogen so far assumed to be environmental. Clin. Microbiol. Infect. 22, 737. https://doi.org/10.1016/j.cmi.2016.05.024.

Rose, C., 1994. Bioaerosols. West. J. Med. 160, 566.

Ruetalo, N., Businger, R., Schindler, M., 2021. Rapid, dose-dependent and efficient inactivation of surface dried SARS-CoV-2 by 254 nm UV-C irradiation. Eurosurveillance 26, 2001718. https://doi.org/10.2807/1560-7917.es.2021.26.42.2001718.

Sakudo, A., Shintani, H., 2010. Sterilization and Disinfection by Plasma: Sterilization Mechanisms, Biological and Medical Applications (Medical Devices and Equipment). Nov. Sci. Publ, New York USA.

Sakudo, A., Shimizu, N., Imanishi, Y., Ikuta, K., 2013. N2 gas plasma inactivates influenza virus by inducing changes in viral surface morphology, protein, and genomic RNA. Biomed. Res. Int. 2013, 694269. https://doi.org/10.1155/2013/694269.

Sakudo, A., Toyokawa, Y., Imanishi, Y., 2016. Nitrogen gas plasma generated by a static induction thyristor as a pulsed power supply inactivates adenovirus. PLoS ONE 11, e0157922. https://doi.org/10.1371/journal.pone.0157922.

Sakudo, A., Toyokawa, Y., Imanishi, Y., Murakami, T., 2017. Crucial roles of reactive chemical species in modification of respiratory syncytial virus by nitrogen gas plasma. Mater. Sci. Eng. C 74, 131–136. https://doi.org/10.1016/j.msec.2017.02.007.

Sánchez-Monedero, M.A., Roig, A., Cayuela, M.L., Stentiford, E.I., 2006. Emission of bioaerosols associated to organic waste management. Ingeniería 1, 39–47.

Sattar, S.A., Ijaz, M.K., 1987. Spread of viral infections by aerosols. Crit. Rev. Environ. Control. 17, 89–131. https://doi.org/10.1080/10643388709388331.

Schindelin, J., Arganda-Carreras, I., Frise, E., et al., 2012. Fiji: an open-source platform for biological-image analysis. Nat. Methods 9, 676–682. https://doi.org/10.1038/nmeth.2019.

Shinya, K., Ebina, M., Yamada, S., Ono, M., Kasai, N., Kawaoka, Y., 2006. Influenza virus receptors in the human airway. Nature 440, 435–436. https://doi.org/10.1038/440435a.

Siegel, J.D., Rhinehart, E., Jackson, M., Chiarello, L., the Healthcare Infection Control Practices Advisory Committee, 2019. 2007 Guideline for Isolation Precautions: Preventing Transmission of Infectious Agents in Healthcare Settings.Available on:Centers Diasease Control Prev (accessed 07/27/2022) https://www.cdc.gov/infectioncontrol/pdf/guidelines/isolation-guidelines-H.pdf.

Sleiman, M., Fisk, W., 2009. Evaluation of mitigation strategies for reducing formaldehyde concentrations in unoccupied Federal Emergency Management Agency-owned travel trailers.Available onCenters Disease Control Prev (accessed 07/27/2022) https://stacks.cdc.gov/view/cdc/26758.

Stephens, B., Gall, E., Heidarinejad, M., Farmer, D.K., 2022. Interpreting air cleaner performance data. ASHRAE J. 64 (3), 20–30.

Takarada, H., Sekine, M., Kosugi, H., Matsuo, Y., Fujisawa, T., Omata, S., Kishi, E., Shimizu, A., Tsukatani, N., Tanikawa, S., Fujita, N., Harayama, S., 2008. Complete genome sequence of the soil actinomycete. J. Bacteriol. 190, 4139–4146. https://doi.org/10.1128/JB.01853-07.

Troko, J., Myles, P., Gibson, J., Hashim, A., Enstone, J., Kingdon, S., Packham, C., Amin, S., Hayward, A., Van-Tam, J.N., 2011. Is public transport a risk factor for acute respiratory infection? BMC Infect. Dis. 11, 16. https://doi.org/10.1186/1471-2334-11-16.

Van Doremalen, N., Bushmaker, T., Morris, D., Holbrook, M., Gamble, A., Williamson, B., Munster, V., 2020. Aerosol and surface stability of SARS-CoV-2 as compared with SARS-CoV-1. N. Engl. J. Med. 382, 1177–1179. https://doi.org/10.1056/NEJMc2004973.

Wang, C., Prather, K., Sznitman, J., Jiménez, J., Lakdawala, S., Tufekci, Z., Marr, L., 2021. Airborne transmission of respiratory viruses. Science 80, eabd9149. https://doi.org/10.1126/science.abd9149.

Williams, A., MacLea, K., 2019. Draft genome sequence of Dermacoccus nishinomiyaensis. Microbiology 8, e01370-19. https://doi.org/10.1128/MRA.01370-19.

Wu, Y., Chen, Y.C., Yu, K., Chen, Y.P., Shih, H., 2015. Deposition removal of monodisperse and polydisperse submicron particles by a negative air ionizer. Aerosol Air Qual. Res. 15, 994–1007. https://doi.org/10.4209/aaqr.2014.08.0166.

Yeh, H., Liu, B., 1974a. Aerosol filtraton by fibrous filters. I: theoretical. J. Aerosol Sci. 5, 191–204.

Yeh, H., Liu, B., 1974b. Aerosol filtraton by fibrous filters. II: experimental. J. Aerosol Sci. 5, 205–217.

Zeng, Y., Manwatkar, P., Laguerre, A., Beke, M., Kang, I., Ali, A., Farmer, D., Gall, E., Heidarinejad, M., Stephens, B., 2021. Evaluating a commercially available in-duct bipolar ionization device for pollutant removal and potential by product formation. Build. Environ. 195, 107750. https://doi.org/10.1016/j.buildenv.2021.107750.

Zhang, D., Murata, K., Hu, W., Yuan, H., Li, W., 2017. Concentration and viability of bacterial aerosols associated with weather in Asian continental outflow: current understanding. Aerosol Sci. Eng. 1, 66–77. https://doi.org/10.1007/s41810-017-0008-y.

Zhao, S., Zhuang, Z., Ran, J., Lin, J., Yang, G., Yang, L., He, D., 2020. The association between domestic train transportation and novel coronavirus (2019-nCoV) outbreak in China from 2019 to 2020: a data-driven correlational report. Travel Med. Infect. Dis. 33, 101568. https://doi.org/10.1016/j.tmaid.2 020.101568.

Zitter, J., Mazonson, P., Miller, D., Hulley, S., Balmes, J., 2002. Aircraft cabin air recirculation and symptoms of the common cold. JAMA 288, 483–486. https://doi.org/10.1001/jama.288.4.483.